Power Performance Improvement of Vertical Axis Wind Turbines by a Novel Gurney Flap Design

Milad Mousavi[1], Mehran Masdari[2], Mojtaba Tahani[3]

Abstract

The aim of this study is to investigate the power performance of vertical axis wind turbines (VAWT) that equipped with diverse gurney flaps. Gurney flaps could increase the aerodynamic efficiency of the airfoils. In this paper, the two-dimensional computational fluid dynamics simulation is used. According to the results, the gurney flap elevate the power coefficient at the low range of tip speed ratio (TSR). Also, it is mentioned that angled gurney flap that has the same aerodynamic performance as standard gurney flap, has the structural excellence and lower hinge moment. Ordinarily, in all gurney flap cases, the power coefficient increases by an average of 20% at the TSR range of 0.6 to 1.8. However, the gurney flap cases do not perform well at the high TSR range and the results show the lower amount of C_p compare to the clean airfoil. The only case that has a higher C_{pmax} than clean airfoil is an angled gurney flap that is applied on the pressure side of the airfoil. This case could increase the C_{pmax} by 25% at the specific TSR. Consequently, the angled gurney flap that is deployed to the pressure side of airfoil could improve the efficiency of VAWT at the particular range of TSR and has structure advantages compare to the standard gurney flap case.

***Keywords**:* Vertical wind turbines, Gurney flaps, Darrieus wind turbine, Power coefficients, Aerodynamic performance, Hinge moment

[1] M.sc Student of Faculty of new sciences and technologies, University of Tehran, Tehran, Iran (Email: m.mousavi.092@ut.ac.ir)
[2] Faculty of new sciences and technologies, Department of aerospace engineering, University of Tehran, Tehran, Iran
[3] Faculty of new sciences and technologies, Department of aerospace engineering, University of Tehran, Tehran, Iran

Nomenclature

C_p	Power coefficient
C_{pmax}	Maximum power coefficient
C_l	Lift coefficient
C_d	Drag coefficient
R	Radius (m)
N	Number of blades
c	Chord (m)
V_∞	Free stream velocity
TSR	Tip speed ratio
C_m	Moment coefficient
ω	Rotational speed (rad/s)
σ	Solidity
h	Gurney flap height (m)
θ	Gurney flap angle
ρ	Density of the air
A	Surface area of the airfoils

1. Main Text

1.1 Introduction

This study is intended to investigate the behavior of darrieus wind turbines equipped with clean NACA 0021 airfoil and airfoil with a gurney flap. The advantages of these turbines (VAWT) are low noise, low manufacture cost, low installation cost, and high-speed efficiency [1].

However, the amount of power coefficient obtained from these turbines is less than horizontal axis wind turbines [2-5]. The output power of four different wind turbines is shown in figure (1).

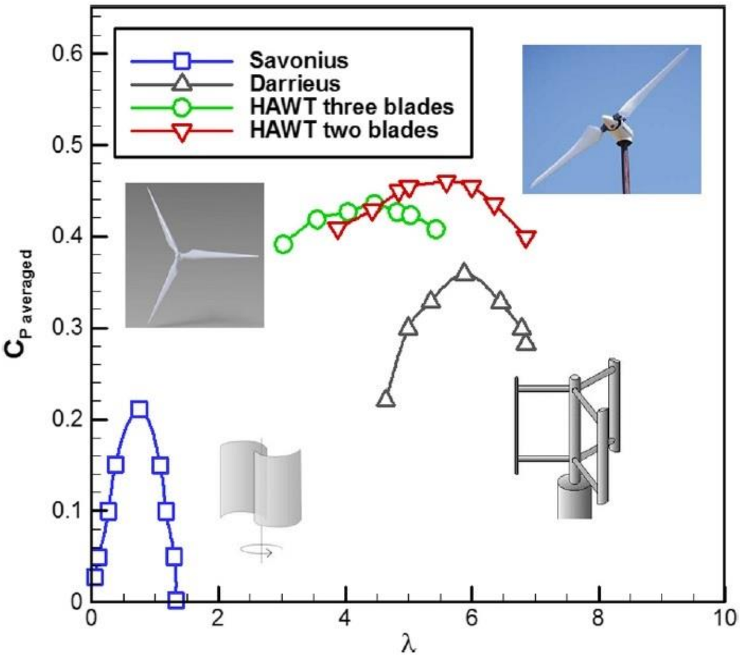

Figure 1. Power coefficients versus TSR produced by four different wind turbines [6]

Another main difference between VAWT and HAWT is the aerodynamic simulation of these turbines. Because of the different angles of attack and various flow velocity direction, predicting the performance of these turbines is difficult [1]. Besides, a lot of complicated flow phenomena such as the dynamic stall, Coriolis and centrifugal forces, aeroelastic effects, boundary layer behavior, flow curvature effects, blade-wake interaction and the shed vortices can make the simulation even harder [7-11].

A comprehensive investigation to achieve the optimized parameters of VAWT such as TSR, Wind speed, solidity, number of blades, and blade shape has been conducted by Ghasemian et al. [6]. Different impacts on the wind farm, aerodynamic noise reduction, dynamic stall control, self-starting characteristics and effects of unsteady and skewed wind conditions have been reviewed. The best results were obtained using the PISO scheme as the solver.

As the results suggested, the higher solidity increase the power coefficient for low TSR. But for the high TSR, the smaller solidity rotors perform better. Accordingly, with increasing the solidity, the TSR operating range has been declined. It was mentioned that the power coefficient is shifted left with increasing the solidity due to the wake effect increase in a narrow passage between blades and the chance of earlier stalling [12].

It was shown that power variation reduces by increasing the blade number. As the blade number is increased, the amount of C_{pmax} could be achieved in lower angular velocities. The smaller number of blades could improve power performance at the higher TSR [13].

It was mentioned that using guide vane is useful especially at the lower wind speeds. Guide vane advantages are minimizing the negative torque, increasing the free stream wind speed and change the flow direction for a better angle of attack of the VAWT blades, and increasing the rotational speed and working hours of the VAWTs [14-16].

Another study is focused on the condition of the flow after the collision to the buildings and urban facilities. It was mentioned that the flow could be skewed, fluctuating, and tilted because of these obstacles. These obstacles could increase the turbulence intensity of the flow and decrease the efficiency of the turbine blades [17, 18].

Some papers are focused on the behavior of flow in wind farms with several wind turbines. The wind speed behind each rotor is reduced but the direction of distributed flow could be more favorable to generate more power in wind turbines. It depends on the lateral velocity and the location pattern of neighboring turbines. Overall, the wind farms can enhance the power generation [19-21].

The noise generated by VAWT was studied in different papers. The noise production of these turbines was divided into two parts. The first part is about aerodynamic forces and the second part is about broadband noises related to the turbulent structures in the wake behind the wind turbine. It was concluded that if the structural optimization applied on the blades and whole coupling system, the generated noise could be lower [22, 23].

Ingham et al [24] was studied the start-up conditions of VAWTs. It was found that in the critical region (TSR<1) the drag plays a significant role on the start-up torque. It was also mentioned that increasing the blade number could make the start-up of the VAWT easier but could decrease the power coefficient. Dynamics stall of blades on the VAWTs was investigated by hau et al [25]. According to the achieved results the stall-onset angle could increase if the non-dimensional numbers like pitch angle and Reynolds increased during the stall on the airfoil.

Another study was focused on the flat deflector which was applied on the free-stream inlet and had a significant effect on the power coefficient. It was mentioned that the free-stream velocity was increased in the near-wake region of the plate, and this could let the turbines perform efficiently [26]. Overlap ratio in VAWTs had a huge impact on starting characteristics than phase shift angle change [27].

The study of applying different airfoils on VAWT was conducted by Subramanian et al [28]. Four different airfoils NACA0012, 0015, 0030 and AIR 001 were considered in this study. NACA 0030 performed better in the low TSR due to the long duration of the attached flow. While NACA 0012 performed better for TSR>1.8 with a broader range of TSR. The shed vortex dissipates much faster for thinner airfoils than thicker airfoils at a higher range of TSR. Two-bladed VAWTs generated more power than three-bladed turbines.

Liebeck drove the first study about gurney flap aerodynamic effects. Various applications of gurney flap were mentioned in this study [29].

A complete research study about all characteristics of gurney flap was conducted by Jain et al. The gurney flap was simulated in six heights between 0.5% to 4% of chord, seven locations from 0% to 20% of chord and seven mounting angles from 30°

to 120°. It was shown that the gurney flap with 1.5% of the chord and 90° mounting angle with the minimum distance from the trailing edge led to the best aerodynamic performance and maximum L/D ratio [30].

In two other studies of gurney flap, the results showed that the gurney flap with a height of 2% of the chord and with a 90° mounting angle is the best choice for aerodynamic performance [31, 32].

Gurney flaps have different applications that recently have been studied. Fan blades [33, 34], compressor blades [32], helicopter rotor [31], micro aerial vehicles (MAV) [35] and vertical wind turbines [36-38] are the latest applications of gurney flaps.

This paper tries to investigate the performance of vertical axis wind turbines equipped with airfoil with gurney flap and compare the results with the clean airfoil. As we could see in the gurney flap reviews the best gurney flap height is 2% of the airfoil chord [31]. Airfoil NACA 0021 is selected for all simulation and the Reynolds number is $2.89 * 10^5$ in all cases because of better performance on VAWTs [39]. The Reynolds number was calculated by the flow velocity that was applied to the inlet boundary.

The innovation point of this study is about using various gurney flaps on the wind turbine blades and make the design of it as easy as it could be to achieve the best performance of the wind turbine.

The first stage of this study is about the investigation of the power performance of each wind turbine in different modes of gurney flap and compare it to the clean airfoil. Then at the second stage, the structural improvement of angled gurney flap is investigated which could be a significant advantage in wind turbine design.

1.1 Methodology

This study trying to use two-dimensional CFD simulation to investigate the behavior of flow around VAWT. ANSYS Fluent is used for simulating the flow fields around the wind turbines.

There are some definitions of VAWT that are important for investigating the performance of wind turbines. Solidity is one of the critical design parameters in VAWT that is calculated as:

$$\sigma = {}^{Nc}/_{R} \tag{1}$$

In equation (1), N is the number of wind turbine airfoils (blades), c is airfoil chord, and R is rotor radius.

Another important design parameter in VAWT is TSR or tip speed ratio and defined as:

$$TSR = {}^{R\omega}/_{V_\infty} \tag{2}$$

In equation (2), R is rotor radius, ω is the angular speed of wind turbine, and V_∞ is free stream velocity.

In all cases, the amount of C_m obtained from the last turbine revolution and the moment coefficient average is calculated. Power coefficient is calculated as:

$$C_m = {Moment}/{0.5.\rho.A.U^2.R} \tag{3}$$

$$C_p = C_m * TSR \tag{4}$$

In this study, the amount of solidity is 0.53 and the TSR range changes between 0.6 and 3. According to the calculation of the inlet flow velocity, the Reynolds number is $2.89 * 10^5$.

As was mentioned in the prior parts, two types of gurney flap are applied on the airfoil. The first one is a standard gurney flap that perpendicular to the airfoil chord. The second one is the gurney flap that has a mounting angle but the vertical axis height is the same as the standard one. Figure (2) shows the geometrical parameters of the gurney flap.

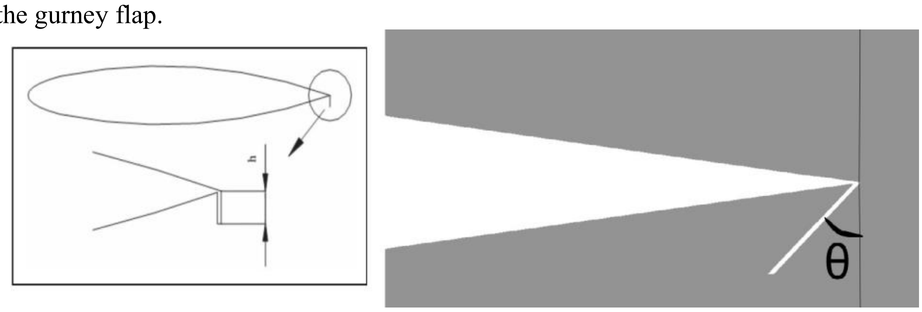

Figure 2. Geometrical parameters of gurney flap

All standard gurney flaps have the height of 2% of airfoil chord and it is the same on the vertical axis of angled gurney flaps. The amount of θ in all angled gurney flaps is 45°.

The boundary condition and domain around the airfoils are illustrated in figure (3). The rotor diameter is 2 m and the airfoil chord according to the validation reference is 0.265 m.

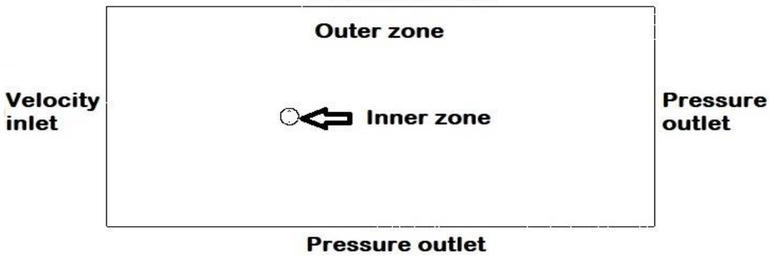

Figure 3. Boundary conditions and domain around VAWT

It is shown in figure (4), we use the sliding mesh method and the domain is separated into two different sections. The outer zone is fixed with unstructured mesh. The inner area rotates with different angular velocity and all airfoils are located there. The inner circle diameter in this study is 3 meters. Correspondingly, the distance between the inlet and the center of the inner zone is 10 rotor diameter and the pressure outlet in the downwind boundary is located 20 rotor diameter from the inner zone circle. The lateral distance between the two pressure outlet boundaries is 40 meters. Around each airfoil, the boundary layer with the appropriate amount of $y^+$is applied. The amount of y^+ around the airfoil is below unity (less than 1).

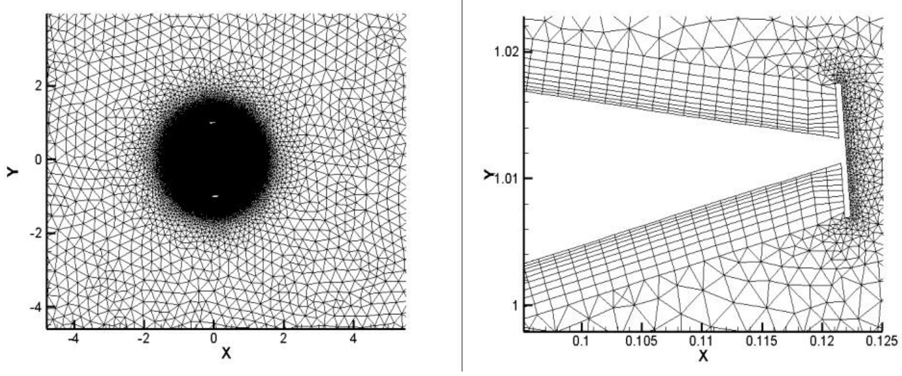

Figure 4. Mesh structure and boundary layer around the airfoil

Ordinarily, the simulation setting was set with the help of various studies [40]. Since the flow is incompressible the pressure-based solver is used and the Coupled algorithm with second-order upwind for space discretization and second-order implicit for time discretization are used [41, 42].

Each case is rotating at least ten revolutions to achieve the constant periodic amount for moment coefficient. After obtaining the constant periodic amount for moment coefficient, the final moment coefficient could be calculated from the average of data in each wind turbine angle. After calculating the average moment coefficient the average power coefficient could be obtained from formula (4). Time steps are selected according to the amount of ω so that it could obtain the result from each 1° rotation.

For turbulence modeling, the $k - \omega\ SST$ model is used. The $k - \omega\ SST$ turbulence model is chosen because of the capability of this model for capturing the flow structures in oscillating domains [43-46]. In this study besides residuals that show the convergence criteria in CFD problems, the velocity and pressure values are other parameters that are confirmed the convergence of the steady simulation [40, 42].

1.2 Validation

To evaluate the accuracy of CFD simulation, the results must compare to the similar experiment test case. In this study, the results of clean darrieus wind turbines compare with the results of Li et al [47]. The comparison of power coefficients of the VAWT without gurney flap in the specific TSR range has been shown at the figure (5).

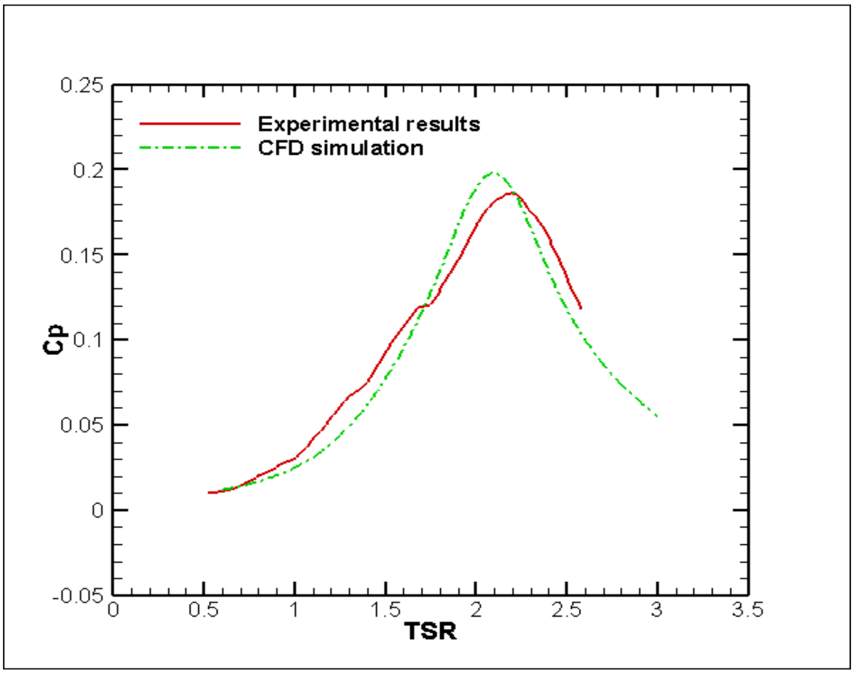

Figure 5. Comparison of power coefficient between experimental results and CFD simulation[47]

According to the results, there is a good correlation between experimental and CFD simulation results and the error percentage of the power coefficient is under 5% in all TSR. In the validation paper, there are many experimental cases with various Reynolds numbers. As was mentioned prior, the Reynolds number of this study is $2.89 * 10^5$ the same as the experiment case and the height of the wind turbine for validation is 2.4 m.

The high amount of solidity in this case, helps the gurney flap improve the amount of power coefficient in the limited TSR [6]. Therefore, a higher amount of solidity makes the wind turbine perform at the limited TSR with a higher power coefficient.

1.3 Structural improvement of applying gurney flap with angle on the pressure side of the airfoil

According to the Masdari et al [48], applying gurney flap on the oscillating airfoil could make structural problems. Gurney flap increases the pressure on the lower surface of the airfoil which makes the flow compressed in the front face of the gurney flap and decreases the speed of the flow. At the same time, this equipment decreases the pressure at the upper surface of the airfoil with two vortexes that rotate at the trailing edge of the airfoil on the opposite direction. Consequently, these two turning vortex structures make the flow over the suction side of airfoil go faster. As these turning vortex structures reduce adverse pressure near the trailing edge, gurney flap decelerates the flow on the lower surface of the airfoil, and makes the pressure rise up. Gurney flaps could increase the aerodynamic efficiency of each airfoil [48].

Ordinarily, the structural design of wind turbines is one of the crucial issues that need much attention. The importance of this section has become more dominant when some fundamental problems like fatigue happen. In this section, two basic cases of the airfoil with gurney flap compare and as the aerodynamic performance of each case is similar to the other, the only advantage is about the structural design.

Consistently, the two significant cases in this section are airfoil with standard gurney flap and angled gurney flap. The vertical axis height of these two cases is precisely the same but the mounting angles are different.

Figure 6 and 7 shows the aerodynamic difference of the two identical case which one of them could make an improvement in the structural prospects [48]. In figure 6 and 7 only the airfoil chord is assumed 1 meter and the NACA 0012 airfoil oscillates in a sinusoidal manner around c/4, and its function is described as $\alpha(t) = \bar{\alpha} + \alpha_0 \sin(\omega t)$. In this equation $\bar{\alpha}$ is mean angle of oscillation, α_0 is the amplitude of oscillation and ω is oscillation speed that came from reduced frequency $k = \frac{\omega c}{2U_\infty}$. The Reynolds number for this case only is $1.07 * 10^5$.

The mounting angle in the angled case is 45° degrees and the vertical height of all cases is 2% of the airfoil chord that is 0.0053 m.

It is shown in figure (6), the lift and drag coefficients are compared and the results show an accurate correlation between the aerodynamic performance of angled and standard gurney flap.

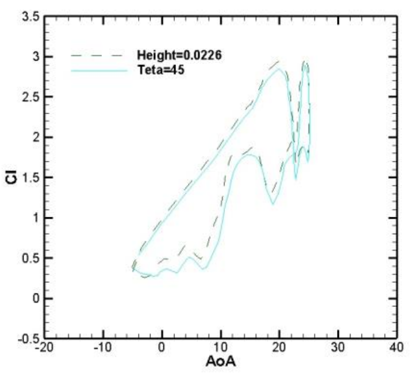

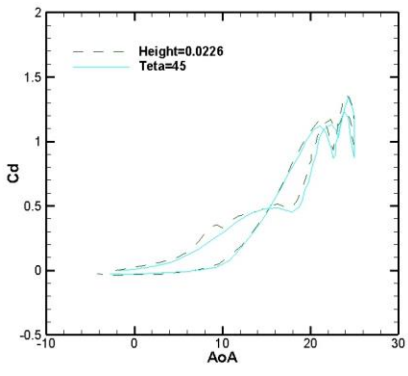

Figure 6. The same aerodynamic performance of standard and angled gurney flap [48]

To demonstrate the structural improvement of the angled gurney flap, we need to calculate the amount of moment coefficient on the connecting point of airfoil and gurney flap. As it is shown in figure (7), the amount of moment coefficient in standard gurney flap is higher. Hence, the higher amount of moment coefficient means bigger loads on the connecting point of the standard gurney flap and more complexity in the design of the airfoil with a gurney flap. More hinge moment, increase the possibility of fatigue or breaking issues on the wind turbine blades.

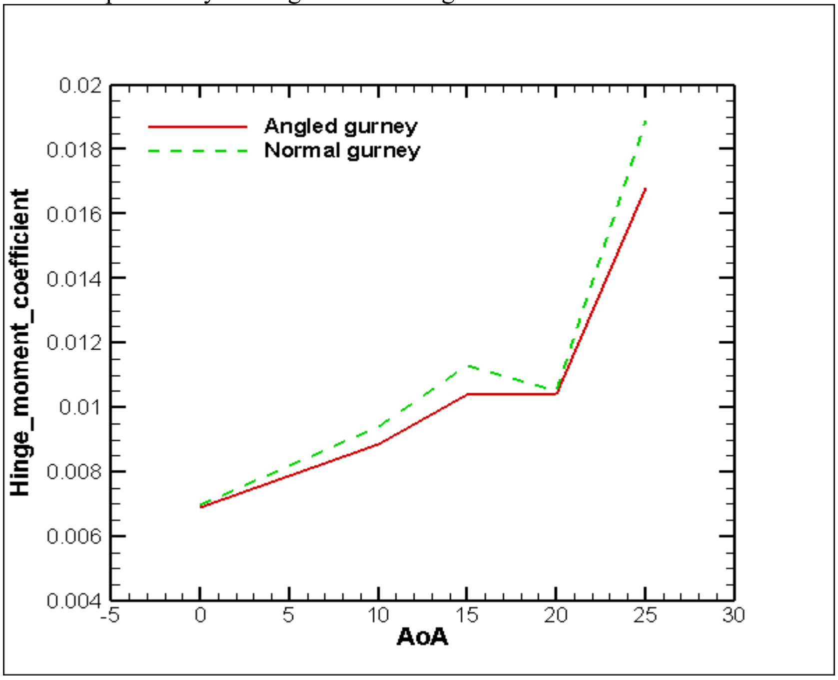

Figure 7. Hinge moment of angled and standard gurney flap [48]

It was mentioned prior, the advantage of the angled gurney flap could be the most important clue to variation of the power performance of VAWT that equipped with angled gurney flap and simpler design in the real world. In the following sections, the position of the gurney flap installation varies and through this, the angled and standard gurney flap cases are compared to each other for further considerations.

1.4 Investigation of gurney flap applying on the pressure side of the airfoil

The first section of this study is about using the gurney flap on the pressure side of the airfoil. The VAWT is with two blades and the basic design parameters were mentioned in the problem statement. Figure (8) shows the geometrical condition of standard and angled gurney flap that is applied on the pressure side.

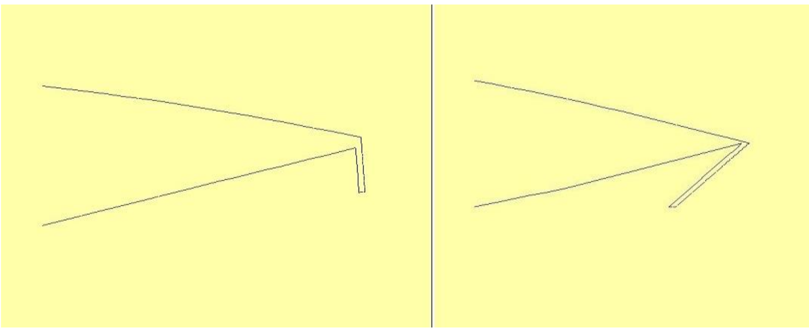

Figure 8. Geometrical condition of standard and angled gurney flap on the pressure side of the airfoil

Accordingly, the gurney flap is applied to the pressure side of the airfoil and three cases are compared and the best performance of the wind turbine is investigated. The first case is a standard gurney flap and the second one is angled gurney flap. These two cases compare with clean airfoil without any gurney flap.

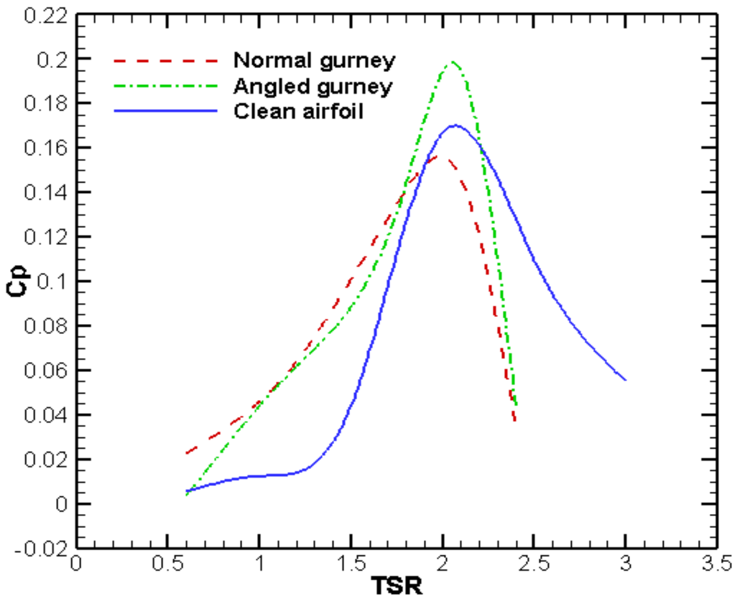

Figure 9. Power coefficient versus TSR at the pressure side case with and without gurney flap

It is shown in figure (9), the performance of angled gurney flap is better than other cases. Ordinarily, there are two separated TSR ranges in figure (9). The first range of TSR is between 0.6 and 2.1 that obviously, the airfoil with gurney flap increases the amount of power coefficient. The second range is between 2.2 and 3 that the gurney flap efficiency is not as well as the clean airfoil case. Therefore, airfoil with a gurney flap could improve the power performance of VAWT at the low range of TSR (0.6 to 2.1). The amount of C_{pmax} is achieved at TSR=2 in almost all cases in this segment.

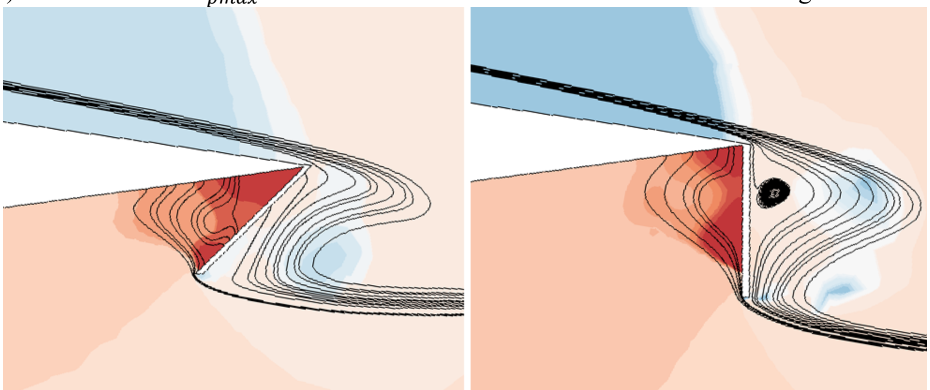

Figure 10. Pressure contour around angled (left) & standard (right) gurney flap on the pressure side [48]

Figure 10 shows the compression of the streamlines around the standard and angled gurney flap. Standard gurney flap has a higher pressure intensity than the angled gurney flap although, higher pressure intensity could elevate the flow force on the front surface of the gurney flap and increase the fatigue in the connecting point of the airfoil and the gurney flap. Furthermore, strong vorticity just behind the standard gurney flap makes the pressure gradient on the upper surface more negative.

As was mentioned prior, the performance of standard and angled gurney flap should be the same but in this case, it is shown that the angled gurney flap increases the maximum power coefficients of VAWT by 25%. Besides, it was shown that the angled gurney flap has an advantage in the structural design since a smaller amount of hinge moment on the airfoil. Using angled gurney flap could improve the performance of VAWT.

Figure 11 and 12 depicts the amount of lift and drag coefficient in various azimuth angles. These results are captured for first blade equipped with gurney flap which applied on the pressure side.

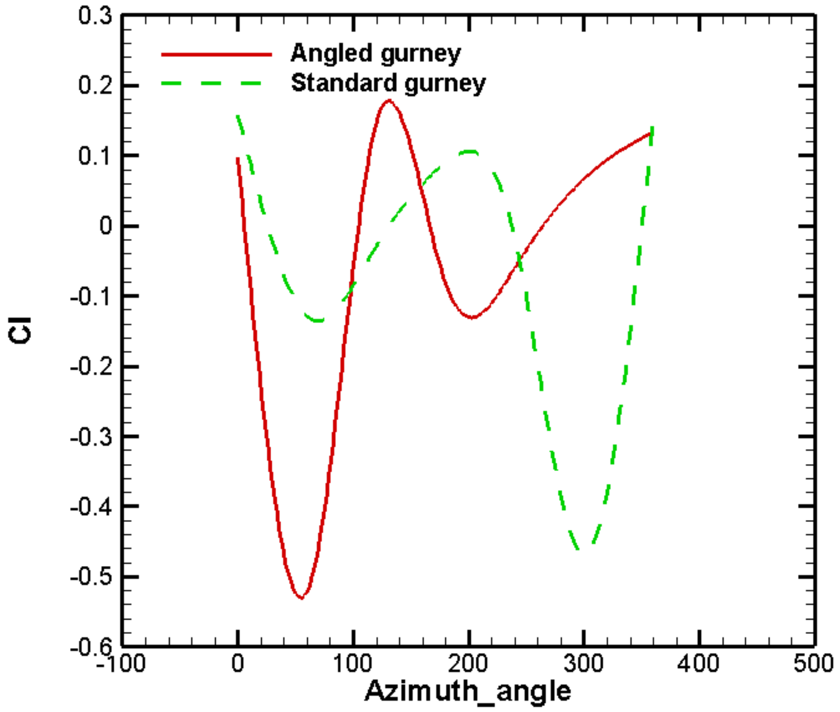

Figure 11. Lift coefficient versus azimuth angle for standard & angled gurney flap on the pressure side at TSR=1.8

Figure 11 illustrates the amount of lift coefficient versus azimuth angle of the same blade. There are some hard fluctuations in the angled gurney flap case which the reason could be the stronger vortexes around the angled gurney flap case. However, the overall figure of the angled and standard gurney flap is similar. The highest difference of the lift coefficient is happened at the 300° azimuth angle with the amount of 0.536.

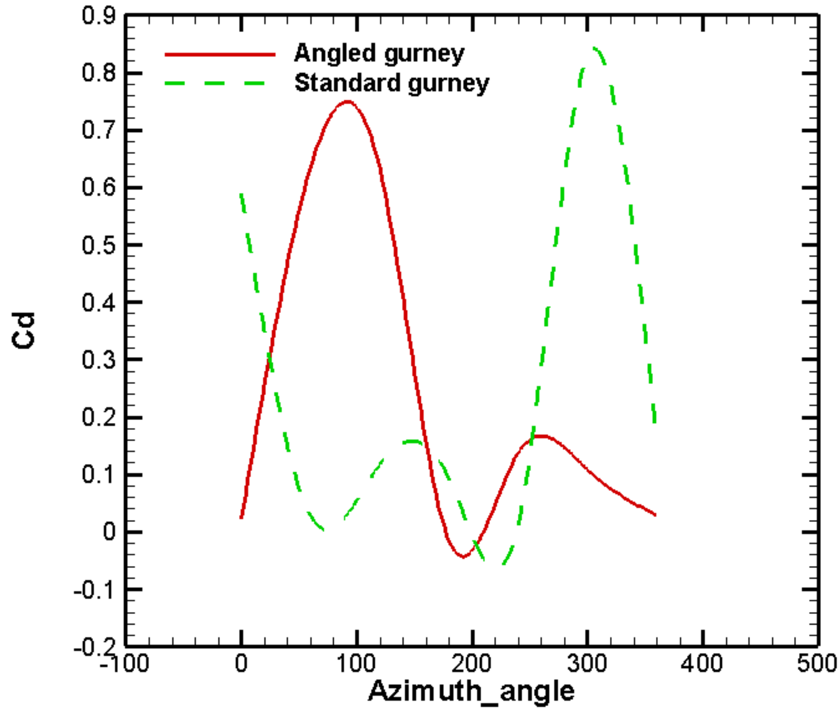

Figure 12. Drag coefficient versus azimuth angle for standard & angled gurney flap on the pressure side at TSR=1.8

Figure 12 illustrates the amount of drag coefficient versus azimuth angle of the same blade. There are some hard fluctuations at 100° azimuth angle in the angled case. The same hard fluctuation is happened at 300° azimuth angle in the standard gurney flap case. The big differences of the angled and standard case could be the result of hard vortex shedding of each airfoil that make the final result less accurate. The highest difference of the drag coefficient is happened at the 300° azimuth angle with the amount of 0.721.

1.5 Investigation of gurney flap applying on the suction side of the airfoil

The second segment of this study is about using the flap on the suction side of the airfoil. The two-bladed VAWT that equipped with two diverse gurney flaps is investigated. Figure (10) shows the geometrical condition of standard and angled gurney flap that is applied to the suction side of the airfoil.

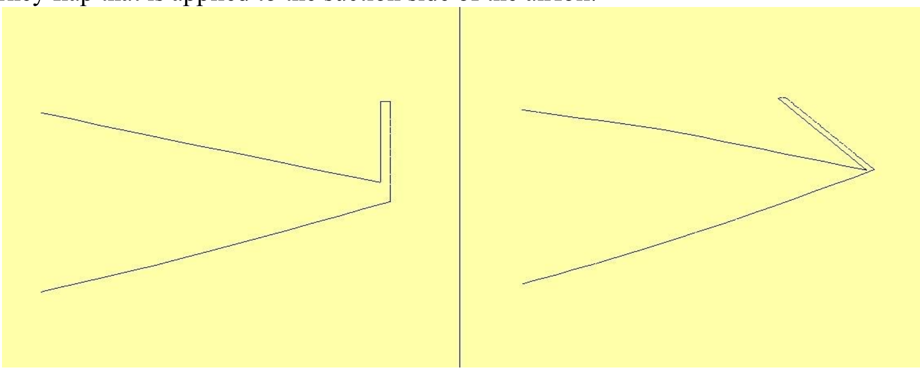

Figure 13. Geometrical condition of standard and angled gurney flap on the suction side of the airfoil

The first case is a standard gurney flap and the other one is angled gurney flap. These two cases compare with clean airfoil without any gurney flap.

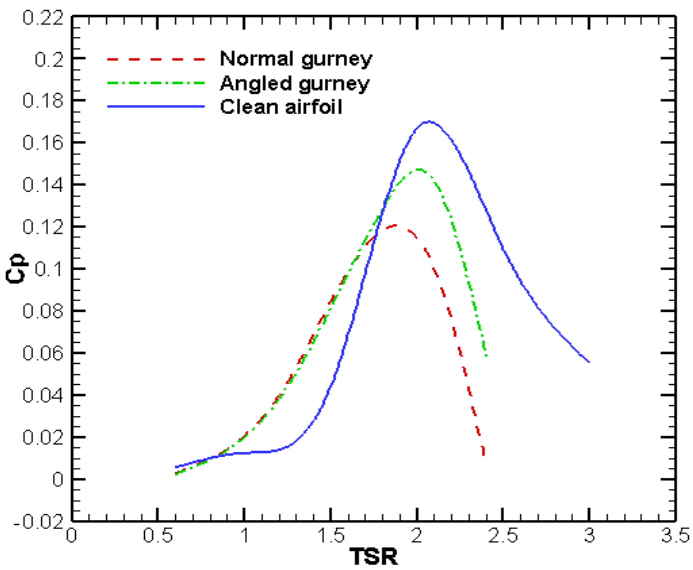

Figure 14. Power coefficient versus TSR at the suction side case with and without gurney flap

Accordingly, the figure (11) shows that applying gurney flap on the suction side of airfoil does not improve the power coefficient of wind turbine except at the low TSR.

Angled gurney flap outperformed especially at the TSR=2. However, the amount of C_{pmax} in two gurney flap cases is lower than clean airfoil but the power coefficient slope at the TSR range of 0.6 to 1.8 is higher than clean airfoil.

Consequently, applying the gurney flap on the suction side of airfoil could not improve the power performance of VAWT as much as using the gurney flap on the pressure side of the airfoil.

Figure 15, 16 depicts the amount of lift and drag coefficient in various azimuth angles. These results are captured for first blade equipped with gurney flap which applied on the suction side.

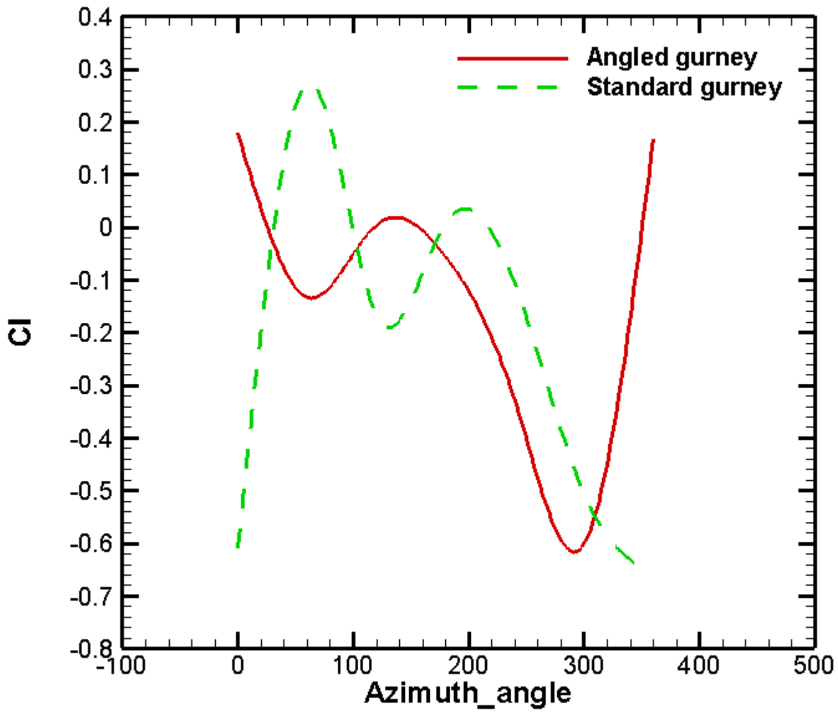

Figure 15. Lift coefficient versus azimuth angle for standard & angled gurney flap on the suction side at TSR=1.8

Figure 15 shows the amount of lift coefficient versus azimuth angle of the same blade. Except at the 60° the amount of lift coefficient of each blade is close. Again at the 360° of azimuth angle there are some big margin between the angled and standard case. The highest difference of the lift coefficient is happened at the 360° azimuth angle with the amount of 0.826.

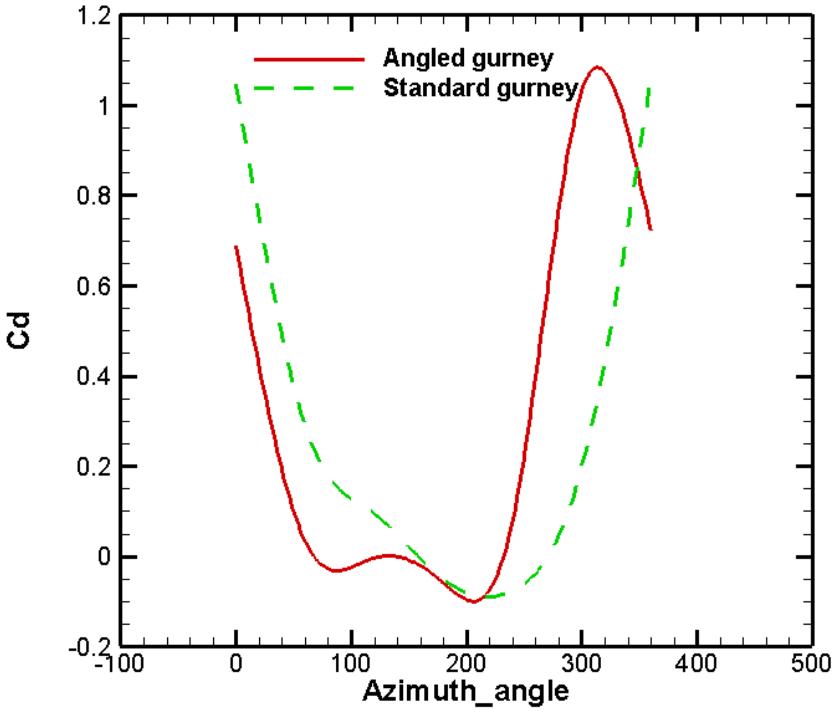

Figure 16. Drag coefficient versus azimuth angle for standard & angled gurney flap on the suction side at TSR=1.8

Figure 16 shows the amount of drag coefficient versus azimuth angle of the same blade. There is a good correlation between the drag coefficient until at 300° azimuth angle. The amount of drag coefficient decreases after 300° in the angled case although, the amount of drag coefficient growth after the same angle. The highest difference of the drag coefficient is happened at the 360° azimuth angle with the amount of 0.342.

1.6 Investigation of the gurney flap applying on both sides of the airfoil

The third part of this study is about using the gurney flap on the both sides of the airfoil. Figure (12) shows the geometrical condition of standard and angled gurney flap that is used on both sides.

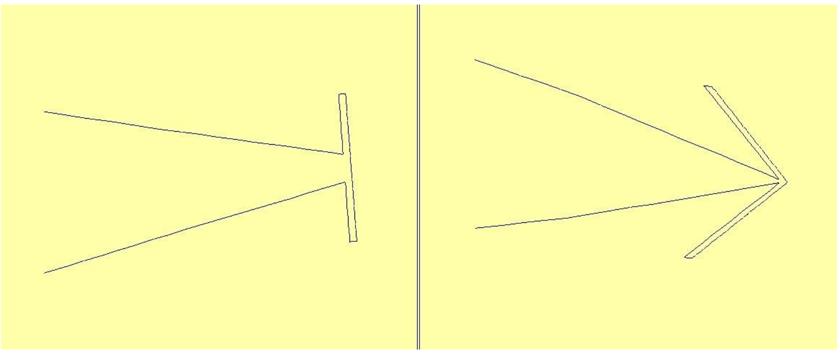

Figure 17. Geometrical condition of standard and angled gurney flap on the both sides of the airfoil

As was mentioned in the last two parts three cases are evaluated and the best case that generates more power is recommended. All design parameters are the same as the prior two parts.

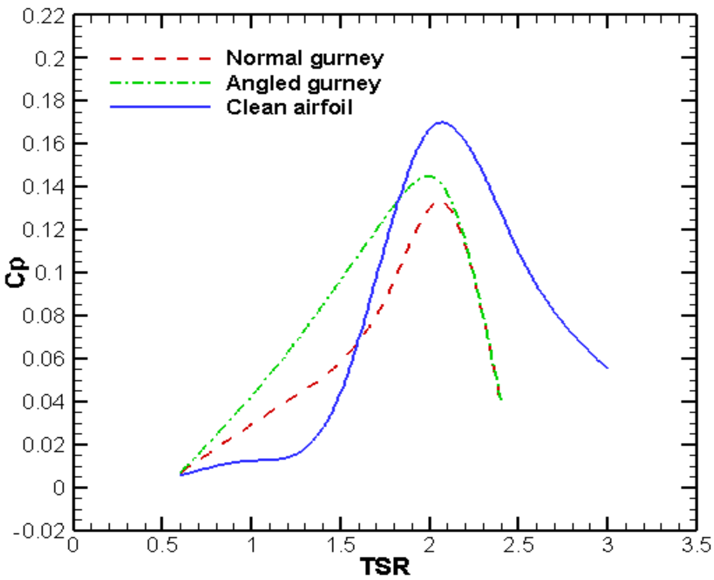

Figure 18. Power coefficient versus TSR at both sides case with and without gurney flap

Accordingly, the performance of angled gurney flap is more efficient than in other cases. The power coefficient slope is higher in the TSR range of 0.6 to 2 than two other cases. However, the maximum power coefficient that is produced at TSR=2 in the clean airfoil case is 20% higher than the angled case. The standard gurney flap as it is shown in figure (13), has the lowest C_{pmax} and the power coefficient slope is higher than a clean airfoil just at the TSR range of 0.6 to 1.5. After the TSR=1.5 in the standard gurney, the amount of C_p is lower than in the other two cases.

The similarity between these three cases is that the amount of C_{pmax} is attained at TSR=2. Consequently, it is obvious that the clean airfoil case is performed better especially at the TSR range of 1.8 to 3 but the angled gurney case has higher C_p at the TSR range of 0.6 to 1.8 than in the other two cases.

Figure 19, 20 depicts the amount of lift and drag coefficient in various azimuth angles. These results are captured for first blade equipped with gurney flap which applied on the both side.

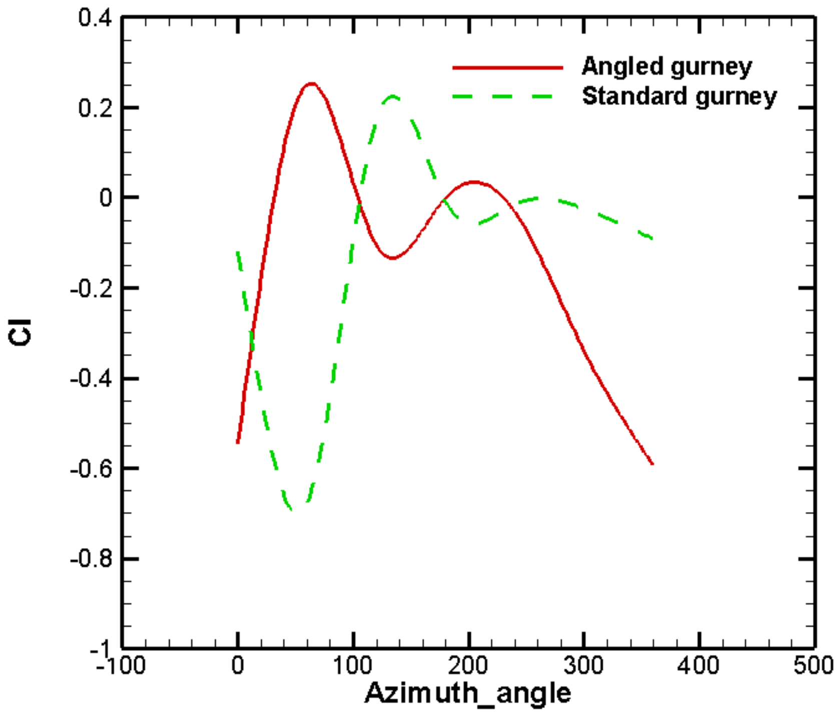

Figure 19. Lift coefficient versus azimuth angle for standard & angled gurney flap on the both side at TSR=1.8

Figure 19 depicts the amount of lift coefficient versus azimuth angle of the same blade. The biggest gap between the results is at the 60° azimuth angle. The results are come close at 200° azimuth angle though, diverged until 360° azimuth angle. The highest difference of the lift coefficient is happened at the 60° azimuth angle with the amount of 0.927.

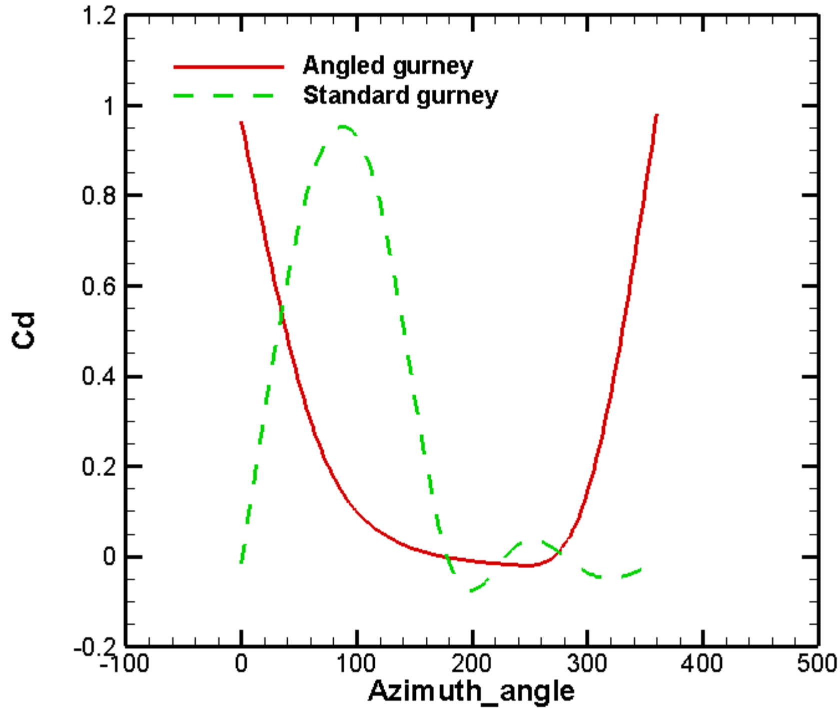

Figure 20. Drag coefficient versus azimuth angle for standard & angled gurney flap on the both side at TSR=1.8

Figure 20 shows the amount of drag coefficient versus azimuth angle of the same blade. Big gaps are shown at the beginning and the end of the angle range. Close results is illustrated around the 200° and 300° azimuth angle. The highest difference of the drag coefficient is happened at the 360° azimuth angle with the amount of 0.995.

1.7 The best mode of gurney flap for VAWTs

Ordinarily, airfoil with gurney flap could enhance the power coefficients at a specific range of TSR. In this segment, the best mode of gurney flap according to the last figure (14) is depicted. Figure (14) illustrates the 7 cases that were compared in the previous parts. Gurney flap that is applied on the pressure side of the airfoil is called gurney in. Gurney flap that is used on the suction side of the airfoil is called gurney out and gurney flap that applied on both sides of the airfoil is called gurney both. The angled gurney flap case in the figure (14) is depicted by the "A" letter and the standard gurney flap without any specific letter.

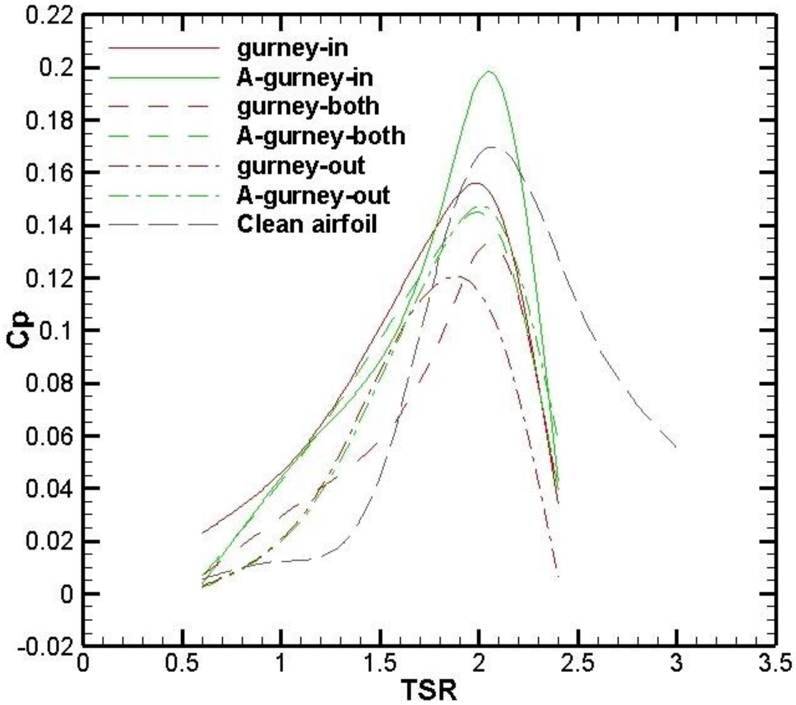

Figure 21. Power coefficient versus TSR in all cases

According to the figure (14), the gurney flap that is applied to the pressure side could elevate the amount of C_p the most. However, between the standard and angled gurney flap that is applied on the pressure side, angled gurney flap is performed more efficiently. Angled gurney flap enhances the amount of C_{pmax} by 25% and besides, angled gurney flap has structural advantages that may alternate the aim of the modeling

The angled gurney flap in all cases enhance the power coefficient more than standard gurney flap and this means more output power and more straightforward design.

1.8 Conclusion

In this study, the effect of the gurney flap that is applied in 3 different locations on the airfoil and with two diverse gurney flap conditions is investigated.

At the first stage of this study, airfoil with standard gurney flap (perpendicular to the chord) and angled gurney flap are compared to each other. The vertical axis height of these two cases is exactly the same but the mounting angles of these cases are different. Accordingly, the results show that the aerodynamic performance of these two cases is similar, however, standard gurney flaps experience higher hinge moment than angled gurney flap on the junction of the airfoil and gurney flap. Therefore, it is concluded that the angled gurney flap case has structural advantages and decrease the possibility of any types of structural issues on the wind turbine blades.

In the second stage, the idea of the first stage is developed on the different locations on the airfoil. Standard and angled gurney flap are applied to the three locations as pressure side, suction side, and both sides of the airfoil NACA 0021.

Gurney flap that is applied to the pressure side of the airfoil could enhance the power coefficients more than other locations. It is mentioned that angled gurney flap could elevate the power coefficient at the low range of TSR (0.6 to 1.8) but it does not perform well at the high range of TSR (1.8 to 3). In this case, the angled gurney flaps outperformed and could enhance the C_{pmax} by 25%.

Gurney flap that is applied to the suction side of the airfoil could not improve the power coefficient of wind turbines except at the low TSR. However, the power coefficient slope at the TSR range of 0.6 to 1.8 is higher than the clean airfoil in this case.

Gurney flap that is applied to the suction side of the airfoil could not improve the power coefficient as well as the gurney flap on the pressure side. Although, the power coefficient slope, in this case, is higher in the TSR range of 0.6 to 2 than two other cases.

Consequently, in almost all cases the gurney flap perform better at the low range of TSR between 0.6 to 1.8 however, at the high range of TSR between 1.8 and 3, the amount of C_p is less than clean airfoil. Angled gurney flap that is applied on the pressure side could elevate the power coefficient slope more than other cases and it is the best case for VAWT.

Therefore, the results show that angled gurney flap cases are performed better than standard gurney flaps since they have the highest amount of power coefficient, highest amount of power coefficient slope, and structural benefits for wind turbine blade.

References

1. Rezaeiha, A., H. Montazeri, and B. Blocken, *Characterization of aerodynamic performance of vertical axis wind turbines: impact of operational parameters.* Energy conversion and management, 2018. **169**: p. 45-77.
2. Eriksson, S., H. Bernhoff, and M. Leijon, *Evaluation of different turbine concepts for wind power.* renewable and sustainable energy reviews, 2008. **12**(5): p. 1419-1434.

3. Govind, B., *Increasing the operational capability of a horizontal axis wind turbine by its integration with a vertical axis wind turbine.* Applied energy, 2017. **199**: p. 479-494.
4. Chong, W.-T., et al., *Cross axis wind turbine: Pushing the limit of wind turbine technology with complementary design.* Applied Energy, 2017. **207**: p. 78-95.
5. Kavari, G., M. Tahani, and M. Mirhosseini, *Wind shear effect on aerodynamic performance and energy production of horizontal axis wind turbines with developing blade element momentum theory.* Journal of Cleaner Production, 2019. **219**: p. 368-376.
6. Ghasemian, M., Z.N. Ashrafi, and A. Sedaghat, *A review on computational fluid dynamic simulation techniques for Darrieus vertical axis wind turbines.* Energy conversion and management, 2017. **149**: p. 87-100.
7. Simão Ferreira, C., et al., *Simulating dynamic stall in a two‐ dimensional vertical‐ axis wind turbine: verification and validation with particle image velocimetry data.* Wind Energy: An International Journal for Progress and Applications in Wind Power Conversion Technology, 2010. **13**(1): p. 1-17.
8. Ferreira, C.S., et al., *Visualization by PIV of dynamic stall on a vertical axis wind turbine.* Experiments in Fluids, 2009. **46**(1): p. 97-108.
9. Tsai, H.-C. and T. Colonius, *Coriolis effect on dynamic stall in a vertical axis wind turbine.* AIAA Journal, 2015. **54**(1): p. 216-226.
10. Amet, E., et al., *2D numerical simulations of blade-vortex interaction in a Darrieus turbine.* Journal of fluids engineering, 2009. **131**(11): p. 111103.
11. Rafiee, R., M. Tahani, and M. Moradi, *Simulation of aeroelastic behavior in a composite wind turbine blade.* Journal of Wind Engineering and Industrial Aerodynamics, 2016. **151**: p. 60-69.
12. Lee, Y.-T. and H.-C. Lim, *Numerical study of the aerodynamic performance of a 500 W Darrieus-type vertical-axis wind turbine.* Renewable Energy, 2015. **83**: p. 407-415.
13. Sabaeifard, P., H. Razzaghi, and A. Forouzandeh. *Determination of vertical axis wind turbines optimal configuration through CFD simulations*. in *International Conference on Future Environment and Energy*. 2012.
14. Chong, W., et al., *The design, simulation and testing of an urban vertical axis wind turbine with the omni-direction-guide-vane.* Applied Energy, 2013. **112**: p. 601-609.
15. Zanforlin, S. and S. Letizia, *Improving the performance of wind turbines in urban environment by integrating the action of a diffuser with the aerodynamics of the rooftops.* Energy Procedia, 2015. **82**: p. 774-781.
16. Nobile, R., et al., *Unsteady flow simulation of a vertical axis augmented wind turbine: A two-dimensional study.* Journal of Wind Engineering and Industrial Aerodynamics, 2014. **125**: p. 168-179.
17. Tabrizi, A.B., et al., *Performance and safety of rooftop wind turbines: Use of CFD to gain insight into inflow conditions.* Renewable Energy, 2014. **67**: p. 242-251.
18. Scheurich, F. and R. Brown, *Vertical-axis wind turbines in oblique flow: sensitivity to rotor geometry.* EWEA Annual event (formerly known as EWEC), 2011.

19. Giorgetti, S., G. Pellegrini, and S. Zanforlin, *CFD investigation on the aerodynamic interferences between medium-solidity Darrieus Vertical Axis Wind Turbines.* Energy Procedia, 2015. **81**: p. 227-239.
20. Barthelmie, R.J. and S. Pryor, *An overview of data for wake model evaluation in the Virtual Wakes Laboratory.* Applied energy, 2013. **104**: p. 834-844.
21. Park, J. and K.H. Law, *Layout optimization for maximizing wind farm power production using sequential convex programming.* Applied Energy, 2015. **151**: p. 320-334.
22. Liu, W., *A review on wind turbine noise mechanism and de-noising techniques.* Renewable Energy, 2017. **108**: p. 311-320.
23. Iida, A., A. Mizuno, and K. Fukudome. *Numerical simulation of aerodynamic noise radiated form vertical axis wind turbines*. in *Proceedings of the 18 International Congress on Acoustics*. 2004.
24. Celik, Y., et al., *Aerodynamic investigation of the start-up process of H-type vertical axis wind turbines using CFD.* Journal of Wind Engineering and Industrial Aerodynamics, 2020. **204**: p. 104252.
25. Hau, N.R., et al., *A critical analysis of the stall onset in vertical axis wind turbines.* Journal of Wind Engineering and Industrial Aerodynamics, 2020. **204**: p. 104264.
26. Kim, D. and M. Gharib, *Efficiency improvement of straight-bladed vertical-axis wind turbines with an upstream deflector.* Journal of Wind Engineering and Industrial Aerodynamics, 2013. **115**: p. 48-52.
27. Kumbernuss, J., et al., *Investigation into the relationship of the overlap ratio and shift angle of double stage three bladed vertical axis wind turbine (VAWT).* Journal of wind engineering and industrial aerodynamics, 2012. **107**: p. 57-75.
28. Subramanian, A., et al., *Effect of airfoil and solidity on performance of small scale vertical axis wind turbine using three dimensional CFD model.* Energy, 2017. **133**: p. 179-190.
29. Liebeck, R.H., *Design of subsonic airfoils for high lift.* Journal of aircraft, 1978. **15**(9): p. 547-561.
30. Jain, S., N. Sitaram, and S. Krishnaswamy, *Computational investigations on the effects of gurney flap on airfoil aerodynamics.* International scholarly research notices, 2015. **2015**.
31. Yee, K., W. Joo, and D.-H. Lee, *Aerodynamic performance analysis of a Gurney flap for rotorcraft application.* Journal of Aircraft, 2007. **44**(3): p. 1003-1014.
32. MDOUKI, R., G. BOIS, and A. GAHMOUSSE, *ENHANCING AERODYNAMIC PERFORMANCES OF HIGHLY LOADED COMPRESSOR CASCADE VIA GURNEY FLAP.*
33. Chen, L., et al., *Experimental and numerical study on the performance of an axial fan with a Gurney flap.* Advances in Mechanical Engineering, 2018. **10**(10): p. 1687814018803804.
34. Hasan Shojaeefard, M. and S. Askari, *Experimental and numerical investigation of the flap application in an airfoil in combination with a cross*

flow fan. International Journal of Numerical Methods for Heat & Fluid Flow, 2012. **22**(6): p. 742-763.
35. Naderi, A., A. Beiki, and B. Tarvirdizadeh, *Numerical investigation of Gurney flap influences on aerodynamic performance of a pitching airfoil in low Reynolds number flow.* Proceedings of the Institution of Mechanical Engineers, Part G: Journal of Aerospace Engineering, 2018: p. 0954410018808708.
36. Zhu, H., et al., *Numerical study of effect of solidity on vertical axis wind turbine with Gurney flap.* Journal of Wind Engineering and Industrial Aerodynamics, 2019. **186**: p. 17-31.
37. Ismail, M.F. and K. Vijayaraghavan, *The effects of aerofoil profile modification on a vertical axis wind turbine performance.* Energy, 2015. **80**: p. 20-31.
38. Bianchini, A., et al., *On the use of Gurney Flaps for the aerodynamic performance augmentation of Darrieus wind turbines.* Energy conversion and management, 2019. **184**: p. 402-415.
39. BOGATEANU, R., et al., *Reynolds number effects on the aerodynamic performance of small VAWTs.* Sci. Bull.–Univ.“Politeh” Bucharest, Ser. D, 2014. **76**(1): p. 25-36.
40. Balduzzi, F., et al., *Critical issues in the CFD simulation of Darrieus wind turbines.* Renewable Energy, 2016. **85**: p. 419-435.
41. Tahani, M., N. Babayan, and A. Pouyaei, *Optimization of PV/Wind/Battery stand-alone system, using hybrid FPA/SA algorithm and CFD simulation, case study: Tehran.* Energy conversion and management, 2015. **106**: p. 644-659.
42. Tahani, M., et al., *A novel heuristic method for optimization of straight blade vertical axis wind turbine.* Energy conversion and management, 2016. **127**: p. 461-476.
43. Ahmadi, S., S. Sharif, and R. Jamshidi, *A numerical investigation on the dynamic stall of a wind turbine section using different turbulent models.* World Academy of Science, Engineering and Technology, 2009. **58**: p. 290-296.
44. Ol, M.V., et al., *Shallow and deep dynamic stall for flapping low Reynolds number airfoils*, in *Animal Locomotion*. 2010, Springer. p. 321-339.
45. Rival, D., G. Hass, and C. Tropea, *Recovery of energy from leading-and trailing-edge vortices in tandem-airfoil configurations.* Journal of Aircraft, 2011. **48**(1): p. 203-211.
46. Castelli, M.R., F. Garbo, and E. Benini, *Numerical investigation of laminar to turbulent boundary layer transition on a NACA 0012 airfoil for vertical-axis wind turbine applications.* Wind Engineering, 2011. **35**(6): p. 661-685.
47. Li, Q.a., et al., *Study on power performance for straight-bladed vertical axis wind turbine by field and wind tunnel test.* Renewable Energy, 2016. **90**: p. 291-300.
48. Masdari, M., M. Mousavi, and M. Tahani, *Dynamic stall of an airfoil with different mounting angle of gurney flap.* Aircraft Engineering and Aerospace Technology, 2020.

Declaration of interests

☒ The authors declare that they have no known competing financial interests or personal relationships that could have appeared to influence the work reported in this paper.

☒The authors declare the following financial interests/personal relationships which may be considered as potential competing interests:

Dr. Masdari and Dr. Tahani are Colleagues in university of Tehran as the supervisor of Mr. Mousavi's M.Sc. thesis.